Identification of heat partition in grinding related to process parameters, using the inverse heat flux conduction model

Eduardo García, Damien Méresse, Iñigo Pombo, Souad Harmand, José
Antonio Sánchez

Identification of heat partition in grinding related to process parameters, using the inverse heat flux conduction model

Eduardo García [a,*], Damien Méresse [b], Iñigo Pombo [a], Souad Harmand [b], Jose Antonio Sánchez [a]

[a] Dpt. Mechanical Engineering, UPV/EHU, Almeda de Urkijo s/n, 48013 Bilbao, Spain
[b] TEMPO EA 4542 Laboratory, UVHC, Carnot Arts Institute, 59300 Valenciennes, France

Abstract

NOMENCLATURE

Parameter	Name	Units
a_e	Depth of cut	mm
A_c	Contact area	m²
A_1	Attempt frequency	s⁻¹
b	Workpiece thickness	mm
h	Convective heat transfer coefficient	W/m²·K
h_{eq}	Equivalent chip thickness	mm
h_1	Reaction constant (Arheninius law)	W/m²·kg
H	Final material hardness	HV
H_1	Hardness of the fully-tempered material	HV
H_3	Hardness fully quenched material	HV
l_c	Contact length	mm
P	Grinding power	W
Q_w'	Specific material removal rate	mm³/mm·s
q_{ch}	Heat flux to the chips	W/mm³
q_{fl}	Heat flux to the fluid	W/mm³
q_t	Total heat flux generated	W/mm³
q_s	Heat flux to the grinding wheel	W/mm³
q_w	Heat flux to the workpiece	W/mm³
R	Molar gas constant	m² ·kg/ s²·K·mol
R_{ch}	Heat Partition to the chips	-
R_s	Heat Partition to the grinding wheel	-
R_{fl}	Heat Partition to the grinding fluid	-
R_w	Heat partition ratio to the workpiece	-
T_M	Absolute Workpiece Temperature	K
T_{amb}	Absolute ambient Temperature	K
U_1	Activation energy for tempering	J/mol
v_f	Infeed speed	mm/min
v_s	Grinding wheel speed	m/s
V'_w	Specific volume of part material removed	mm³/mm
ε	Emissivity	-
κ	Thermal conductivity	
ψ	Probability of tempering	-
σ	Stefan-Boltzmann Constant	W/m²K⁴

ABSTRACT

Grinding is an abrasive machining process characterized by producing high quality components for high added-value industries. Thermal damage is an undesired phenomena that may ruin nearly finished products. The study of thermal damage requires understanding the mechanisms of heat partition between wheel and workpiece. In this work and original methodology and experimental set up for the study the influence of grinding variables on the heat partition to the workpiece, R_w, is presented. The new methodology avoids errors related to the steep thermal gradients typical of grinding operations. In addition, uncertainty related to the actual area of contact is suppressed thanks to a rigid and controlled experimental configuration. An inverse model based on Levenberg-Marquardt algorithm and a finite element model has been used for heat partition to the workpiece identification. Results have lead to a time-dependant R_w definition which had not been previously proposed in literature, and they have allowed as well relating variations in R_w values to physical removing mechanisms of grinding. Results have been validated by means of an indirect parameter: workpiece hardness variation during the tests, which strengthens the validity of the results.

1. INTRODUCTION

Grinding is an abrasive machining process characterized by producing high quality components for high added-value industries (aerospace, energy, tooling...) in terms of tight dimensional tolerances and smooth surface roughness. By contrast, grinding is also characterized by requiring a high amount of energy input per unit volume of material removed. This energy is turned into heat in the contact zone and can cause excessive heating of the workpiece leading to thermal damage on its surface [1]. Thus, the occurrence of thermal damage becomes one of the limiting constraints of productivity in grinding technology.

Increasing material removal rate is limited by the apparition of workpiece burn. The classic solution for burning problems is the use of cooling fluids but their effect is limited. Hence researches try to improve cooling effect by refrigerating the coolant [2] or improving their convective effect [3] . However, these advances are not enough for avoiding burning in some cases. Therefore, understanding the mechanisms that govern workpiece temperature increase and relating them to industrial process parameters become a key factor for grinding process control and optimization.

It is assumed that the power consumed by the grinding wheel spindle is transformed into heat in the contact zone. This heat is evacuated through four ways: workpiece, wheel, ground chips and cooling fluid. The partition of this heat that goes into the workpiece, R_w, is the cause of workpiece temperature increase and thermal damage [4]. Therefore its determination is very important for process optimization. However, it is a

parameter difficult to assess since it depends on a large number of parameters: tribological, mechanical and geometrical. In fact, on shallow grinding with Al_2O_3 wheels scientific literature give values between 0.25 and 0.85.

Usually, authors have identified R_w by matching temperature data experimentally obtained with calculated temperature from theoretical models. One of the main limitations of this methodology, and one of the causes of the wide dispersion of R_w above, is the steep thermal gradients (up to 1000K/s [5]) found in the contact zone, that limit the reliability of the measured temperatures.

For obtaining the theoretical temperature modelization of the process is necessary. Initially, the grinding wheel heating was modeled as a rectangular moving heat source along a semi-infinite body [5]. Analytical models [7], [8], [9] have allowed to highlight some behaviors of the rubbing contact like the triangular shape of the generated heat flux. These were progressively replaced by numerical models with the rapid increase of calculation power. As it is gathered in [10], numerical models are used following similar approaches, workpiece discretization, effect of grinding wheel as a moving heat source and consideration of the convective effect of cooling fluid; but differ in four main aspects: geometry of heat source (rectangular vs triangular), contact length estimation, material properties (constant or not with temperatures), and 2D or 3D models. This way, Brosse [11] used finite element methods and thermography to characterize the distribution of R_w in the contact zone finding the triangular or the parabolic shape of the heat fluxes provided more accurate results.

Following the approach above described, Kohli found values in the range 0.6-0.75 for shallow grinding with Alumina wheels [5]. He used the Jaegers [6] solution with a triangular heat flux shape. Hadad studied grinding with Minimum Quantity of Lubrication-MQL [12]. Based on analytical models found in [9], his experiments concluded that R_w varies between 0.73 and 0.77 for grinding with MQL, 0.82 for dry grinding and the use of cooling fluid reduced R_w to 0.36.

Inverse methods are numerous and widely used to study various heat transfer phenomena [13]. Recently, the function specification method was used by Meresse to get heat flux repartition on a disc in braking conditions [14]. Ludowski used the Levenberg-Marquardt method [15] to get the thermal boundary conditions in heat exchangers [16]. The conjugated gradient method with adjoint problem has been used by Luchesi to identify a moving heat source in machining conditions [17].
Inverse methodology has already been used in grinding to determine R_w by matching experimental temperature with and an output numerical data, the nodal temperature at the sensor location, and minimizing the error. Three inverses analyses are used in [18] to obtain R_w, the geometry of the heat source, and the convection coefficient h_f from temperature data. Experiments are described in [19] and authors have found R_w values in the range 0.70 and 0.74 for grinding with Al_2O_3 wheels using hardened steel and plain carbon steel. More recently, Hong has presented the assessment of R_w using a finite

element method as direct model but results have not been validated by experimental data [20]. Anderson performed this work for shallow and deep grinding. For the assessment of workpiece temperature distribution they used the finite elements method, and took into account the material removed by deleting elements in the model for the case of deep grinding. They estimated heat partition ratios to the workpiece by matching numerical results to those obtained with an infrared camera measurements obtaining R_w in the range 0.8-0.85. Results match those obtained by the model developed by Rowe [9].

The objective of this paper is to provide an original methodology and experimental set-up that contribute to a better understanding of the influence of grinding variables on the heat partition ratio R_w. With respect to existing literature, the new methodology eliminates the errors induced by the steep thermal gradients that occur in grinding operations. Uncertainty related to the actual area of contact between both bodies (wheel and workpiece) is also suppressed by using a rigid and controlled geometrical configuration. Assessment of R_w in shallow grinding of hardened steel with Al_2O_3 wheels, and its relation with actual grinding parameters is presented in this paper using an inverse heat conduction model. Grinding tests are developed in the so-called On-Machine Test Bench, an alternative experimental set-up that allows reproducing grinding conditions while accurate temperature measurements and control of contact area are possible. The transient heat conduction problem is solved by a finite element model which takes into account the workpiece material removal during the process. The heat partition to the workpiece is identified by matching temperature data from thermocouple measurement to nodal temperature of the finite element model. The R_w parameter is identified with the Levenberg-Marquardt algorithm. Validation of temperature measurements is indirectly carried out by metallurgical analyses, which consists of measuring the micro-hardness of the tested samples and comparing it to the analytical model proposed in [21]. Results have led to a time-dependent definition of R_w which had not been previously proposed in literature; in addition it has been possible to relate the observed variations of R_w to the physical material removing mechanisms of grinding.

2. GRINDING PROCESS

As it has been mentioned, in grinding, for practical issues it is accepted that all the energy consumed in the grinding wheel spindle is transformed into heat in the contact zone. Therefore, the total heat flux generated in the contact zone, q_t, can be obtained from equation 1, where P is the power consumption in the grinding wheel spindle. The partition of this heat that is evacuated through the workpiece, R_w, and the heat flux directed to the workpiece can be obtained from Equation 2.

$$q_t = \frac{P}{b \cdot a_e} \qquad \text{Eq.1}$$

$$q_w = \frac{R_w \cdot P}{b \cdot a_e} \qquad\qquad \text{Eq.2}$$

An experimental test bench is developed to reproduce this machining process and to get temperature data close to the contact zone. A thermal finite element model describing the heat conduction through the workpiece is then defined to allow the identification of the heat flux boundary condition by an inverse method.
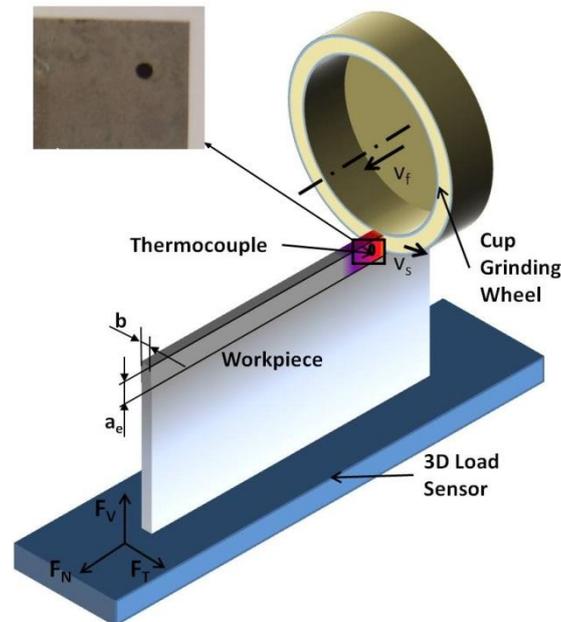
2.1. Experimental Test Bench

Figure 1 – Experimental Test Bench description

The experimental work was developed in the new test bench configuration shown in Figure 1. A horizontal-spindle CNC surface grinding machine is used for the study. A cup wheel, with a constant spinning speed, carries out grinding of a static workpiece plate. The wheel removes material by moving towards the workpiece at a constant infeed speed, v_f. Insulating PTFE (Teflon) plates are placed at both sides of the steel plate to minimize heat losses to the clamps. The actual relative velocity between abrasive and workpiece is equal to the wheel spinning speed. This disposition presents some advantages compared to traditional grinding tests developed in grinding machines. The area of contact between wheel and workpiece, which is the area whereby heat enters the workpiece, is constant and known at every moment. In the direction of the spindle axis the configuration is very rigid, so that the effect of machine deformations can be neglected and the actual equivalent chip thickness, effectively controlled. Finally, continuous heat flux to the workpiece in the contact zone produces progressive heating of it, so that high temporal thermal-gradients are avoided and temperature can be accurately measured with thermocouples.

A Power meter device Load Controls Inc. UPC-FR installed on the wheel spindle and a Kistler 9257B dynamometer are also used for power and force measurement. Here

experimental tests are performed with AISI4140 hardened steel (630HV). The workpiece is a rectangular prism of 100mm length x 5mm width x 45mm height. A hole is machined by EDM on the side of the workpiece and a K-type thermocouple of 200μm diameter is welded inside by capacitive discharge to track the temperature evolution. The hole is 1mm in diameter and is placed 3.5mm far from the edge of the workpiece, and 2.5mm in depth. Due to machining and welding alignment errors, the positioning of thermocouples is submitted to an uncertainty that has been estimated to be under 0.4mm.

2.2. Finite element model

Heat generation on the ground surface and heat diffusivity in the workpiece are modeled using the finite element method. ANSYS 13.0 is used for its ability to solve the heat equation for 3D transient problems and to take into account the steel removal during the process. The insulating PTFE plates are also included in the model in order to take into account non negligible heat losses. Material properties of the two materials have been considered constant and are listed in Table 1.

	AISI 4140 Steel	PTFE (Teflon)
Thermal Conductivity [W/m·K]	52	0.28
Specific Heat [J/kg·K]	500	1000
Density [kg/m³]	7800	2140

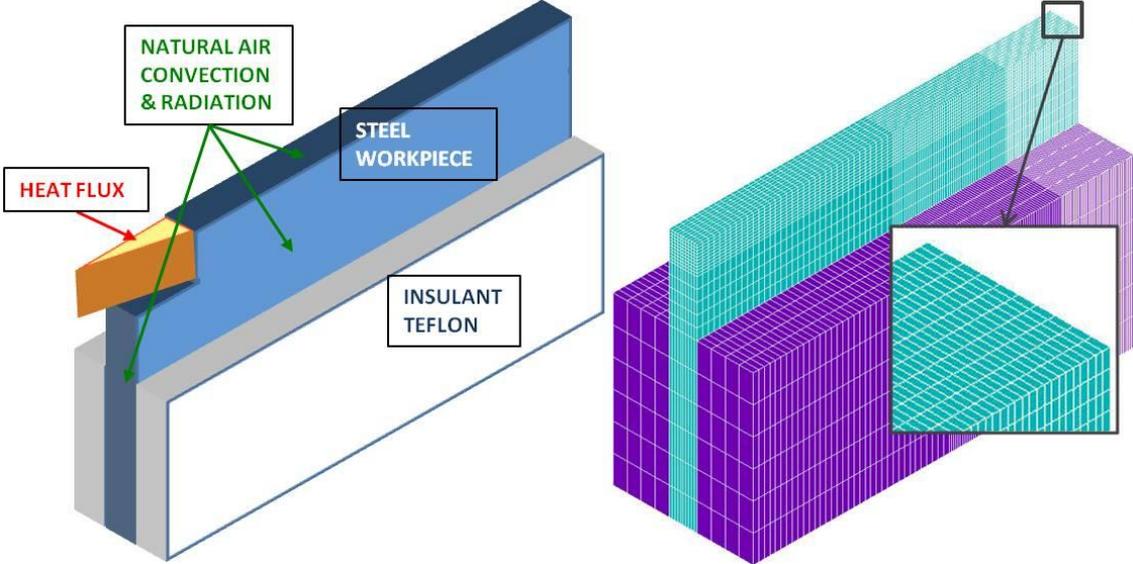Table 1 – Materials thermal properties in finite element model

Figure 2 - Boundary conditions and meshing of the 3D finite element thermal model

Boundary conditions are presented on Figure 2. To simulate the heat generation on the ground workpiece surface, a moving heat source is used. For a correct definition of this

boundary condition the amount of heat flux entering the workpiece and its distribution over the contact area is needed. This area is theoretically defined by the product of the contact length l_c and the wheel width b. Due to uncertainties related to the nature of deformations that must still be tackled, the value of l_c considered in grinding varies from the geometrical contact length l_g [4][11], up to values that can be 2 to 3 times higher [22]. In this case, thanks to our experimental configuration, the l_c is equal to the width of the workpiece, b, and thus the contact area can be determined as the product of the workpiece width b and the depth of cut a_e (eq.3):

$$A_c = b \cdot a_e \qquad\qquad \text{Eq.3}$$

The rate at which the energy is generated is approximately proportional to the rate of material removal. Taking into account the triangular geometry of the undeformed chip thickness, a triangular distribution has been chosen for the heat source [7][9]. This way, eq. 4 expresses the heat flux to the workpiece as a function of the distance to the left face of the workpiece, x:

$$q_w = R_w \cdot q_t \cdot \frac{(b - x)}{b} \qquad\qquad \text{Eq.4}$$

A perfect contact is considered between the workpiece and the insulating material as described by the equation eq. 5. On workpiece free areas, heat losses by convection and radiation are modeled corresponding to the equation eq.6. The heat convection parameter h depends on the workpiece nodal temperature and on the room temperature T_{amb}. A correlation of natural convection for vertical plate in laminar flow is used as described by the equation eq.7. Within the working conditions the heat transfer coefficient has been estimated to vary between 10 and 40W/m². A sensitivity study was developed using the limit values of h. Results show that maximum workpiece temperature, whose value is close to 1300K, only decreases 11K when increasing h from 10 to 40W/m². The low impact of convective parameter h in maximum workpiece temperature has led to consider a constant h value of 20W/m².

$$k \left(\frac{\partial T_N}{\partial n}\right)_{workpiece} = k \left(\frac{\partial T_N}{\partial n}\right)_{teflon} \quad \text{and} \quad T_N^{workpiece} = T_N^{teflon} \qquad\qquad \text{eq. 5}$$

$$-k \left(\frac{\partial T_M}{\partial n}\right)_{open} = h(T_M - T_{amb}) + \varepsilon\sigma(T_M^4 - T_{amb}^4) \qquad\qquad \text{eq. 6}$$

$$h = 1.42 * \left(\frac{|T_M - T_{amb}|}{L}\right)^{0.25} \qquad\qquad \text{eq. 7}$$

With regard to radiation losses, it has to be mentioned that usually thermal grinding models do not include radiation because of its negligible influence [10]. However, due to the singularities of this test configuration, high temperatures were encountered in the vicinity of the contact zone (over 1300K in some cases), which motivated taking radiation heat losses into account. The value of the emissivity is set to 0.6 commonly used for medium carbon steel. A low influence of the emissivity has also been highlighted by simulations.

The model was meshed using eight nodes prism-shaped elements with a single degree of freedom, temperature, at each node. It can be seen on figure 2 that the mesh was refined near the contact zone. For the selection of the smallest element size in this area a sensitivity study was developed. 0.2mm, 0.05mm and 0.01mm element sizes were tested in this study. The maximum temperature difference between the 0.2mm model and the 0.01mm was 6%, however, the calculation time was increased notoriously, from 7min of the 0.02mm elements model to more than 7h for the 0.01mm elements model. Thus, 0.02mm was consider accurate enough for the issue of the study

Finally, since the depth of cut during the test is not negligible, material removal was simulated using the element death feature built into ANSYS. In [23] this tool was used for modeling deep grinding. This feature does not actually remove the elements, but deactivate them by applying a severe reduction factor to their conductivity.

The solution of a test is obtained by incrementally stepping the heat flux along the workpiece. For each step the heat source moves the length of an element (0.2mm), and at the same time the precedent element is eliminated. Taking into account that the ground length is 2mm each test simulation consists of 11 steps. The time of each step is determined by the infeed speed of the grinding wheel v_f.

The FEM has been completed with a model for simulating tempering. As it has already been explained, measuring temperatures in grinding is a very difficult task. From the previous explanation it becomes evident that the experimental set-up is characterized by low thermal gradients, which reduces errors in temperature measurement. Even though, in order to increase soundness of results, it is proposed here to use redundant data from indirect temperature measurement, as that provided by hardness alterations. Taking into account the high temperatures suffered by the workpiece, metallurgical transformations (such as tempering) are expected to occur during the test.

For its simulation a tempering model based on the formulation of Fedosheev [21] has been implemented. The input of the model is the temperatures of the FEM and it calculates the loss of hardness due to tempering by using the concept of probability of tempering ψ:

$$\frac{d\psi}{dt} = h_1 \cdot (1 - \psi)^3 \qquad \text{Eq. 8}$$

with h_1 given by:

$$h_1 \equiv A_1 \exp\left\{-\frac{U_1}{R \cdot T_M}\right\}$$

Eq. 9

The differential equation [eq. 8] has been transformed in a discrete equation [eq. 10] taking advantage of the step by step solution of the transient thermal problem:

$$\varphi_{i+1} = \varphi_i + \Delta t \cdot h_1 \cdot (1-\psi)^3$$

Eq.10

The final hardness H of the steel after tempering will be given by the following equation:

$$H = H_3 - (H_3 - H_1) \cdot \psi$$

Eq.11

3. INVERSE METHOD FOR THE HEAT PARTITION PARAMETER IDENTIFICATION

The identification of the heat partition to the workpiece, R_w, is possible thanks to reliable experimental temperature measurements and to an accurate thermal model. Knowing all the boundary conditions except R_w, an inverse method is used to evaluate this parameter value. The Levenberg-Marquardt algorithm is used to match the experimental value of the temperature with the numerical estimation at the sensor location. This iterative method has been largely applied to inverse heat transfer problems because of its stability and its accuracy [16]. It consists of the minimization of quadratic functional $S(R_w)$ where R_w can be a scalar or a vector. Minimizing $S(R_w)$ is performed by equating to zero the derivative of $S(R_w)$ with respect to R_w (eq.12).

$$\nabla S(Rw) = 2 * J(Rw) * [T_{exp} - T_{num}(Rw)]$$

Eq.12

$$J(Rw) = \begin{bmatrix} \dfrac{\partial T_1}{\partial Rw_1} & \cdots & \dfrac{\partial T_1}{\partial Rw_j} & \cdots & \dfrac{\partial T_1}{\partial Rw_N} \\ \cdots & \cdots & \cdots & \cdots & \cdots \\ \dfrac{\partial T_i}{\partial Rw_1} & \cdots & \dfrac{\partial T_i}{\partial Rw_j} & \cdots & \dfrac{\partial T_i}{\partial Rw_N} \\ \cdots & & \cdots & & \cdots \\ \dfrac{\partial T_N}{\partial Rw_1} & \cdots & \dfrac{\partial T_N}{\partial Rw_j} & \cdots & \dfrac{\partial T_N}{\partial Rw_N} \end{bmatrix}$$

Eq.13

The Jacobian $J(R_w)$, also called the sensitivity matrix, defines the sensitivity of the temperature at time step i to a variation of the parameter R_w at the time step j (eq.13). This is a N*N matrix for time-dependent R_w parameter. For constant parameter R_w, J is a vector and its length corresponds to the number of simulated time step N. In case of time-dependent R_w value with one value per time step, the Jacobian J becomes a N*N matrix.

The technique consists of correcting the values of the unknown vector R_w by solving the direct finite element model and applying a variation on values according to the sensitivity coefficients. This is an iterative method as the algorithm converges progressively on the optimal solution with several iterations. The variation on R_w values is applied thanks to the following formula (eq.14):

$$Rw^{k+1} = Rw^k + J^k * \left[T_{exp} - T_{num}\left(Rw^k\right)\right] * \left[\left(J^k\right)^T * J^k * \left(1 + \mu^k\right)\right]^{-1} \qquad \text{Eq.14}$$

The damping factor μ^k is useful to allow the convergence on the optimal R_w value because it reduces oscillations and instabilities for an ill-conditioned problem. However the damping factor introduces a bias on the parameter estimation. This is progressively decreased with the iterations when the convergence is obtained on the optimal parameter value so as to be negligible on the final iteration. More details on the Levenberg-Marquardt method can be found in the literature [15]. Two stopping criteria have been defined. The iterative algorithm is stopped when the calculated R_w variation is lower than $\Delta R_w = 10^{-3}$ between two iterations. Otherwise, the identification is stopped if the number of iterations has reached $nb_{max-it} = 8$.

Numerical case was developed to assess the feasibility of the R_w identification. Experimental temperature data are simulated by setting heat flux boundary condition in the range of the dissipated power in a real grinding test. Nodal temperature data is exported at the sensor location and the identified R_w value is compared to the previously imposed in the direct model. This study was performed with a constant R_w value (R_w =0.65) and time-dependent R_w. Results are presented for this second case on the figure 3. The convergence is rapidly obtained for the constant R_w value (2-4 iterations) depending on the initial guess. For time-dependent R_w, 6-7 iterations are necessary to get negligible temperature residuals. For the presented case, a good agreement can be observed between the imposed and identified R_w values. The temperature residual is lower than 1K on the entire temperature profile.
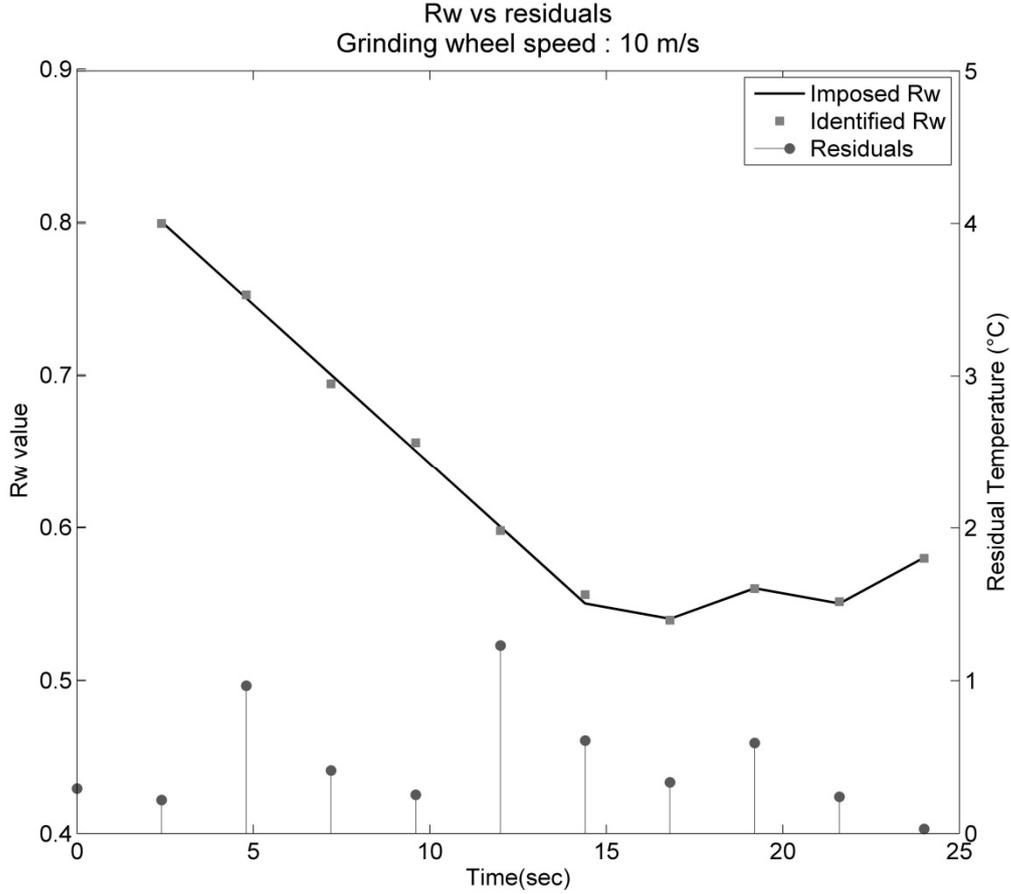
Figure 3 – Inverse method numerical validation

4. RESULTS

4.1. R_w values of tested configurations

Experimental tests and then R_w parameter estimations were performed for two types of abrasive wheels (2A46I8VWEB2 and 30SA46I8VWEB2) and five values of specific material removal rates Q_w' by varying the infeed speed v_f (eq.15).

$$Q_w' = l_c \cdot v_f \qquad\qquad \text{eq. 15}$$

The grinding wheels selected have a similar configuration but differ in the type of alumina used. The 2A46I8VWEB2 wheel is composed of fused alumina grits, while in the case of 30SA46I8VWEB2 the Sol-Gel 3M™ Cubitron™ 321 alumina type is used. For facilitating identification of the wheels through the text the following nomenclature is used

 – Wheel 1 = 2A46I8VWEB2 (fused alumina)
 – Wheel 2 = 30SA46I8VWEB2 (Sol-Gel 3M™ Cubitron™ 321 alumina)

Q_w' varies from a very low value (Q_w'=0.083mm³/mm·s) to typically met value in grinding finishing operations (Q_w'=1.25mm³/mm·s). The equivalent chip thickness h_{eq} is

deduced by dividing Q_w' by the grinding wheel speed v_s. The process parameters values are gathered in Table2. The low Q_w' values of the Test 1 and 2 correspond to very low values of h_{eq} where ploughing is predominant. These values have been selected in order to assess the influence of the different material removing mechanisms in heat partition. The specific volume of part material removed, V_w', is small: 10mm³/mm, in order to avoid the effect of wear of the abrasive grits.

Test	Q_w' [mm³/mm s]	h_{eq} [nm]	v_f [mm/min]	v_s [m/s]	V_w' [mm³/mm]
1	0.083	4	1	24	10
2	0.17	7	2	24	10
3	0.42	18	5	24	10
4	0.83	35	10	24	10
5	1.25	53	15	24	10

Table 2 - Process parameters values

Figure 4 and 5 shows the results obtained for test 2 and 4 of Table 2 using Wheel 1 and Wheel 2, respectively. The evolutions of both, experimental and simulated temperature, as well as the value of the heat partition to the workpiece are plot. Regarding the experimental temperature, it must be noted that the measured signal is very stable and its increase is gradual (gradients below 100K/s). This is an important advantage for the accuracy of the results face to the conventional grinding tests. One of the problems of the thermal test in grinding is that the temperature varies so fast (10000K/s, in some cases [5]) that the thermocouple is not able to accurately measure it. As it can be noticed from Figures 4 and 5, errors related to this effect are minimized.

For the assessment of R_w, two approaches were followed. Initially, R_w was assumed to be constant along the test, but as it can be seen in Figures 4 and 5 the numerical (circular dots) and the experimental temperatures (continuous line) do not match properly. After 3-4 iterations, the algorithm converges to a solution but residuals are not negligible and the difference between the numerical and the experimental temperature can reach 100K. As a consequence, a second approach was followed, which consisted of considering R_w as a time-dependent parameter.

The results obtained with the time-dependent R_w, matched almost perfectly with the experimental temperature being the residuals negligible. Paying attention to the evolution of R_w along the test it can be seen that it follows a similar behavior in both figures. The value of R_w is higher at the beginning of the test and decreases to a stabilized value as the test goes on. For Test 2, h_{eq} =7nm, its value starts at 0.72 and rapidly decreases to 0.55 (Figure 4). After 20sec, R_w looks to be stable until the end of the test (54sec). In Test 4, h_{eq}=35nm, the initial value is higher (0.86) and tends to stabilize around 0.66. This behavior has been observed in all tested conditions.

This effect has not been previously described in scientific literature. The hypothesis for its explanation relies on the transient behavior of the abrasive grits at the beginning of use after the dressing operation. The dressing operation sharpens the abrasive grits, so that they recover their cutting ability. Sharp corners on the surface of the grits involve much reduced contact surfaces between abrasive grains and workpiece. Due to the extreme brittleness of alumina (which is a ceramic material) these sharp edges suffer a very fast microscopic wear shortly after the grinding operation starts. This effect is well-known in grinding practice [1]. After this short transient period, wear stabilizes and the operation progresses with a much lower wear rate. Therefore, during the transient period the actual area of contact for heat conduction increases until the regime of stable wear is reached. The growth of a metallic third body on the contact interface during the transient period [24] may also have an influence on heat partition. Future work will include microscopic observation of the surface of the abrasive grits at different instants of the transient period, in order to validate the above hypotheses.
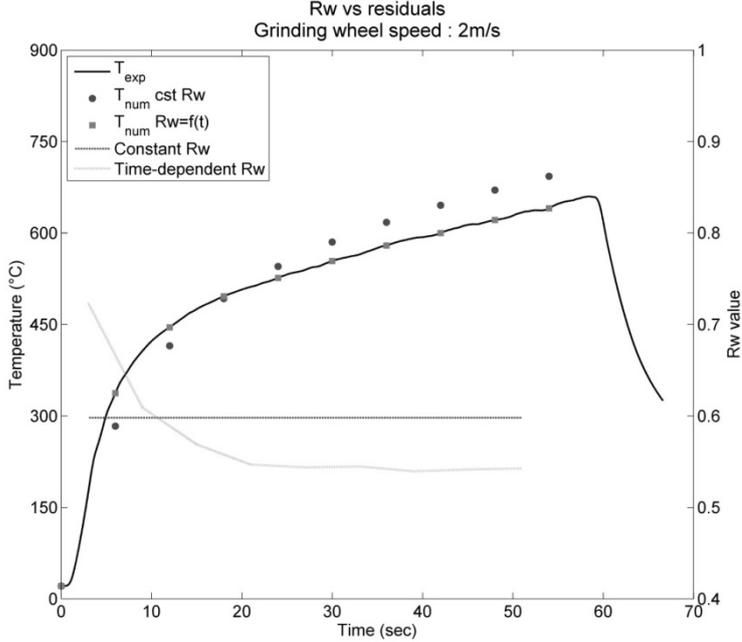

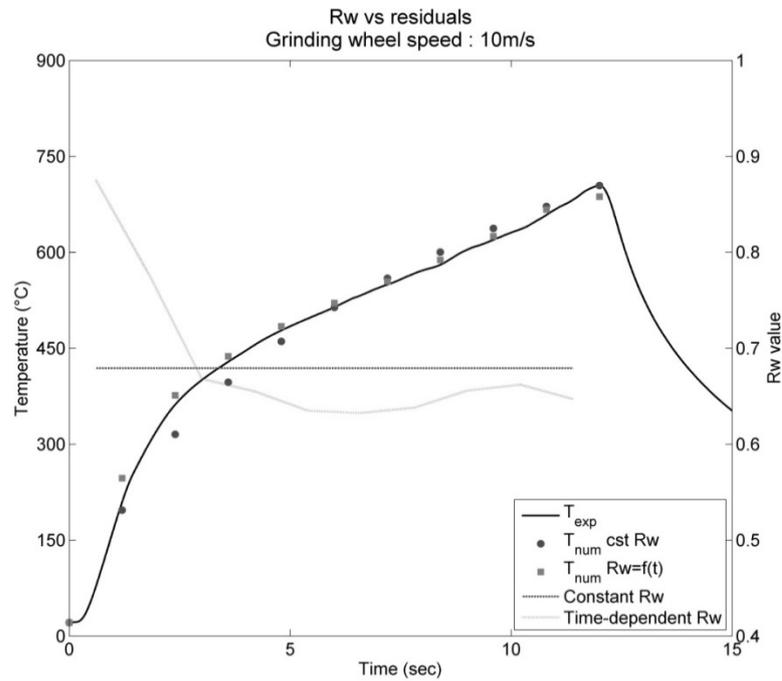Figure 4 – Temperature and estimated R_w value for h_{eq}=7nm – Wheel 1

Figure 5– Temperature and estimated R_w value for h_{eq}=35nm – Wheel 2

Taking the above assumption into account the stabilized phase of the test is more representative of the grinding conditions found in an industrial process, due to the shortness of the unsteady part.

Figure 6 shows the values of R_w at the stable phase as a function of h_{eq} for all tested conditions. Clear differences can be observed between Test 1 and 2 (low values of h_{eq}, 4-7nm) and the others. For low values of h_{eq} (4-7nm), the part of the consumed energy directed to the workpiece is around 53% of the total. By contrast, for higher h_{eq} (18-53nm), R_w values are identified in the range of 0.7-0.8. This trend has been identified for the two abrasive materials tested.

This difference is related to the different predominant mechanism of material removing (rubbing, ploughing and shearing) [25] as a function of h_{eq}. At low depths of cut (h_{eq} = 4 and 7nm), the abrasive grits hardly penetrate the workpiece. This leads to high plastic deformations (ploughing is predominant) and, consequently, a non-negligible part of the power is consumed mechanically, the assumption that all consumed energy is transformed into heat is not fulfilled. Increasing the grit penetration with a higher equivalent chip thickness implies that grits are able to remove the material by shearing it. The plastic strains become less important, all energy can be assumed to be transformed into heat and consequently the part of the consumed energy directed as heat to the workpiece is higher.
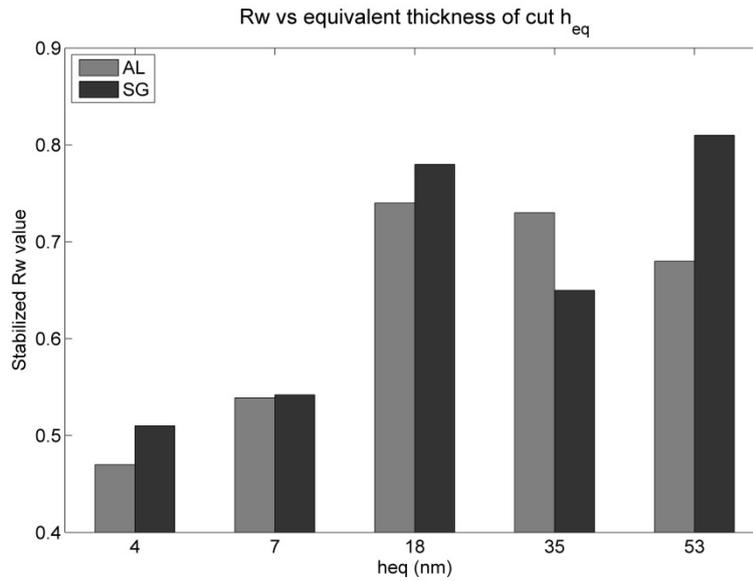
Figure 6– Stabilized R_w value as the function of the equivalent chip thickness h_{eq}

It has been possible to determine this effect thanks to the tight control of h_{eq} (not achievable in conventional grinding tests) and to the accurate temperature measurements. Separation of ploughing and shearing effects in real grinding is not possible since the grit passes through both phases during its contact with workpiece material. Thus, the separated contribution of ploughing and shearing has not been addressed before.

During the contact of the grit with the workpiece chip thickness, h_{cu}, varies, from a minimum (ploughing predominant) to a maximum (shearing predominant) in up grinding, or vice versa in down grinding. This assumption would imply that as long as the chip thickness varies R_w so should vary too, as it is shown in Figure 7

4.2. Uncertainty on the sensor location

An analysis is realized to determine the error on the R_w value regarding the uncertainty on the sensor location. Because of closeness of the thermocouple on high thermal gradient area, an error on the position could induce an important error on R_w value. The inverse method is then performed by choosing another node in the model close the initial node. The location is varying in the three directions for a value of +/-0.4mm. This procedure allows simulating a different sensor location unless another experimental test. For each condition, it gives eight optimization calculations. Results are showed on Figure 7 for 3 experimental tests. The uncertainty study is only performed for time-dependent R_w and is plotted regarding the material removal volume. For the 3 configurations, we observe a more significant uncertainty span at the beginning. This span reaches +/-0.05 on the first time step but rapidly decreases with the material

removal. After a removal of 10 mm^3, it becomes under +/- 0.02. Besides it can be noticed that the tendency of R_w to decrease with material removal for each condition.
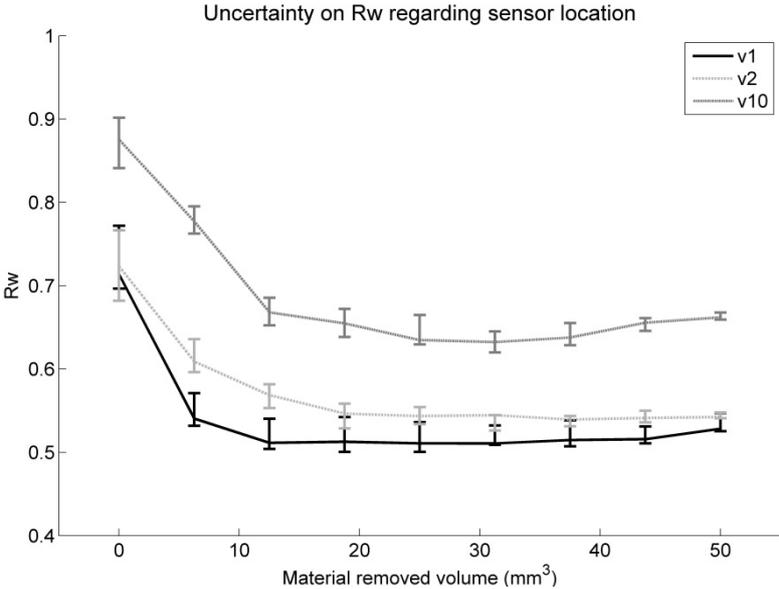

Figure 7 – Error on R_w values regarding uncertainties on thermocouple location

4.3. Validation of Temperature Measurements by Micro-Hardness Evaluation

The validation consists of comparing the hardness of the workpiece near the contact zone after the test, to the theoretical hardness obtained from the tempering model, described in Section 2.2. Since tempering is temperature and time dependant phenomena, if the final hardness is similar it can be deduced that the temperature history is the same. For the assessment of the theoretical hardness the temperature evolution of the FEM with the identified time-dependant R_w is used.

The parameters used in equations 9-11 for the calculation of hardness are: U_1 is in the range of 80 – 90kJ/mol according to tempering curves in [26]. The value of the attempt frequency A_1 is set to 10000s^{-1}. The fully-tempered H_1 and the fully quenched materials H_3 have a hardness of 300 and 730HV respectively. The initial hardness value H_0 has been measured on each workpiece before the experimental test.

Figure 8 shows the comparison for the Test 3 using Wheel 1 along the length direction. Two zones can be clearly seen: the rehardened zone close to the friction zone and the tempered zone. In this case, the deviation between the simulated and the measured curves of micro-hardness is below 5%. Although it is evident, it must be reminded that in the region on the left hand side of the re-hardening curve has occurred due to very high temperatures. Therefore the model for hardness prediction used at this point is no longer valid.
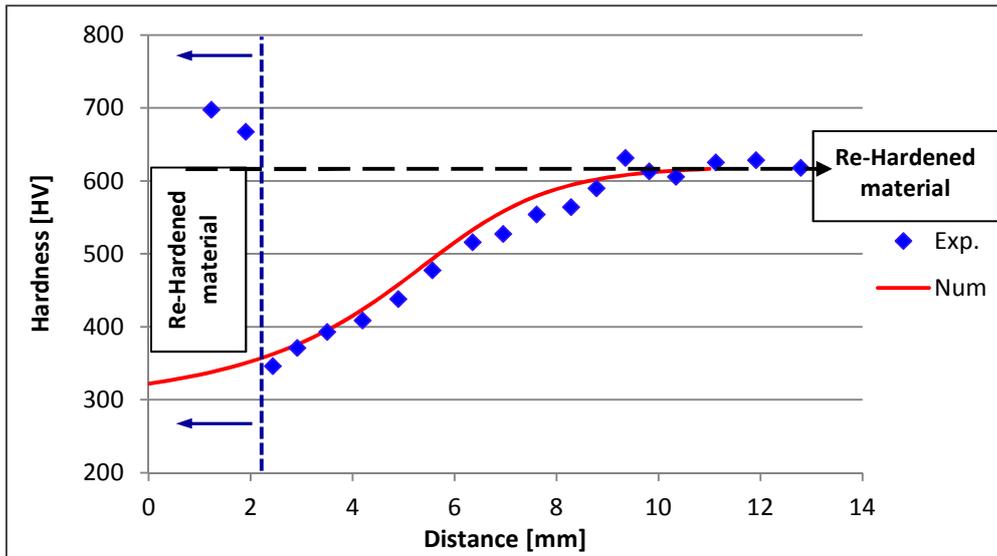
Figure 8 - Experimental vs simulated hardness for h_{eq}=18nm – Wheel 1

Table 3 gathers the maximum and mean deviations between the measured hardness and the theoretical hardness obtained with the model using the variable R_w. In the worst case, the upper limit of the deviation punctually reaches 20% and the maximum difference is under 10% for mean values. This is an acceptable result taking into account the dispersion in micro-hardness measurements. This metallurgical study tends to confirm the results obtained for the R_w values and the efficiency of the methodology.

Qw' [mm³/mm s]	heq [nm]	2A46I8VWEB2		30SA46I8VWEB2	
		Mean	Max.	Mean	Max.
0.083	4	5.39%	13.43%	9.37%	20.05%
0.17	7	4.95%	9.35%	5.44%	13.26%
0.42	18	2.38%	5.05%	3.82%	13.67%
0.83	35	1.70%	6.42%	3.59%	6.78%
1.25	53	9.58%	18.23%	3.54%	11%

Table 3 - Maximum and mean deviations between theoretical and measured hardness values

5. CONCLUSIONS

In this paper an original methodology and experimental set-up that contribute to a better understanding of the influence of grinding variables on the heat partition ratio R_w has been introduced. From the work carried out, the following conclusions can be drawn:

- With respect to existing literature, the new methodology eliminates the errors induced by the steep thermal gradients that occur in grinding operations. Experimental results showed that heating of the workpiece is progressive, and

the temperature increase in the workpiece is not so steep (100K/s), compared to the 10000K/s that can be found in conventional grinding tests. In addition, uncertainty related to the actual area of contact between both bodies (wheel and workpiece) is also suppressed by using a rigid and controlled geometrical configuration.

- Results have led to a time-dependent definition of R_w which had not been previously proposed in literature. In all tested conditions a similar behavior is observed: high R_w initial values that decrease to stabilized smaller values. Initial values range from 0.9 to 0.75 depending on h_{eq}, descending to stabilized values between 0.7 and 0.5, respectively. This behaviour could be due to local variations on the contact surfaces as a consequence of abrasive grits wear and to the apparition of a third body.

- For cutting conditions were the chip thickness (h_{eq}) is very small (4-7nm), the predominant material removing mechanism is ploughing, and results show that R_w varies between 0.50 and 0.55. By contrast, when the depth of cut is increased (chip thickness > 15nm) the prevailing material removing mechanism is shearing. Under these conditions the R_w is between 0.7 and 0.8. In the bibliography, there is no mention to the effect of material removing mechanism in R_w. The justification is that from all the energy available in the contact when ploughing is predominant a non negligible part of it is consumed in plastic deformations, whereby less amount of the consumed energy is transformed into heat and directed to the workpiece.

- A metallurgical study offers the possibility of comparing the numerical temperature with the experimentally reached temperature, by means of a indirect parameter: hardness. The theoretical hardness profile along the workpiece thickness matches micro-hardness measurements (mean deviations between predicted and measured hardness on the range 9.5-1.5%). This implies that the temperature field obtained numerically after R_w identification is accurate enough and is able to predict the subsurface steel hardness after a grinding operation.

- Future work will include microscopic observation of the surface of the abrasive grits at different instants of the transient period, in order to optically identify the growth of the flat wear areas and the appearance of a third body that validates the above hypotheses of the time-dependant R_w.

References

[1] S. Malkin, C. Guo, Grinding Technology, Industrial Press Inc, 2008.

[2] Y. Gao, S. Tse, H. Mak, An active coolant cooling system for applications in surface grinding, Applied Thermal Engineering. 23 (2003) 523–537.

[3] J.-Z. Zhang, X.-M. Tan, B. Liu, X.-D. Zhu, Investigation for convective heat transfer on grinding work-piece surface subjected to an impinging jet, Applied Thermal Engineering. 51 (2013) 653–661.

[4] S. Malkin, R.B. Anderson, Thermal Aspects of Grinding: Part 1—Energy Partition, J. Eng. Ind. 96 (1974) 1177–1183.

[5] S. Kohli, C. Guo, S. Malkin, Energy Partition to the Workpiece for Grinding with Aluminium Oxide and CBN Abrasive Wheels, Journal of Engineering for Industry. 117 (1995) 160.

[6] J.C. Jaeger, Moving sources of heat and the temperature of sliding contacts, J. and Proc. Roy. Soc. New South Wales. 76 (1942) 202.

[7] C. Guo, S. Malkin, Analysis of energy partition in grinding, Journal of Engineering for Industry. 117 (1995) 55–61.

[8] A.S. Lavine, An exact solution for surface temperature in down grinding, International Journal of Heat and Mass Transfer. 43 (2000) 4447–4456.

[9] W.B. Rowe, Thermal analysis of high efficiency deep grinding, International Journal of Machine Tools and Manufacture. 41 (2001) 1–19.

[10] D.A. Doman, A. Warkentin, R. Bauer, Finite element modeling approaches in grinding, International Journal of Machine Tools and Manufacture. 49 (2009) 109–116.

[11] A. Brosse, P. Naisson, H. Hamdi, J.M. Bergheau, Temperature measurement and heat flux characterization in grinding using thermography, Journal of Materials Processing Technology. 201 (2008) 590–595.

[12] M. Hadad, B. Sadeghi, Thermal analysis of minimum quantity lubrication-MQL grinding process, International Journal of Machine Tools and Manufacture. 63 (2012) 1–15.

[13] Thermal measurements and inverse techniques, CRC Press, Boca Raton, FL, 2011.

[14] D. Meresse, S. Harmand, M. Siroux, M. Watremez, L. Dubar, Experimental disc heat flux identification on a reduced scale braking system using the inverse heat conduction method, Applied Thermal Engineering. 48 (2012) 202–210.

[15] D.W. Marquardt, An Algorithm for Least-Squares Estimation of Nonlinear Parameters, SIAM Journal on Applied Mathematics. 11 (1963) 431.

[16] P. Ludowski, D. Taler, J. Taler, Identification of thermal boundary conditions in heat exchangers of fluidized bed boilers, Applied Thermal Engineering. 58 (2013) 194–204.

[17] V.M. Luchesi, R.T. Coelho, An inverse method to estimate the moving heat source in machining process, Applied Thermal Engineering. 45-46 (2012) 64–78.

[18] Guo, C., Malkin S., "Inverse heat transfer analysis of grinding. PartI: Methods". Journal of Engineering for industry, (1996), Vol. 118/137-142.

[19] Guo, C., Malkin S. "Inverse heat transfer analysis of grinding. PartII: Applications". Journal of Engineering for industry, (1996b), Vol. 118/143-149.

[20] K.. Hong, C.. Lo, An inverse analysis for the heat conduction during a grinding process, Journal of Materials Processing Technology. 105 (2000) 87–94.

[21] O.B. Fedoseev, S. Malkin, Analysis of Tempering and Rehardening for Grinding of Hardened Steels, Journal of Engineering for Industry. 113 (1991) 388–394.

[22] I.D. Marinescu, W.B. Rowe, B. Dimitrov, I. Inasaki, Tribology of abrasive machining processes, William Andrew Pub., Norwich, NY, 2004.

[23] D. Anderson, A. Warkentin, R. Bauer, Experimental validation of numerical thermal models for dry grinding, Journal of Materials Processing Technology. 204 (2008) 269–278.

[24] Godet, M. The third body approach: mechanical view of wear, Wear 100 (1984) 437–452.

[25] P. Rosenthal, N.S. Eiss, Discussion: "On the Mechanics of the Grinding Process Under Plunge Cut Conditions" (Hahn, R. S., 1966, ASME J. Eng. Ind., 88, pp. 72–79), Journal of Engineering for Industry. 88 (1966) 79.

[26] ASM International, Carbon and alloy steels, ASM International, Materials Park, OH, 1996.